Estimating the effects of ENSO upon the observed freshening trends of the western tropical Pacific Ocean

Awnesh Singh[1] and Thierry Delcroix[1]

Received 9 September 2011; accepted 10 October 2011; published 8 November 2011.

[1] A significant surface freshening trend and an eastward expansion of fresh surface waters have been documented in the western tropical Pacific, consistent with the expected effects of climate change. The highest El Niño Southern Oscillation (ENSO) variability in Sea Surface Salinity (SSS) has been also documented in that region, with different quantitative signatures for the Eastern and Central Pacific ENSO events (EP and CP ENSO, respectively). This study hence analyses to what extent have the EP and CP ENSO events contributed to the long-term freshening trends, relying on 1955–2008 in situ SSS data and on EP and CP ENSO main features. We show the influence of EP ENSO events to be negligible, while CP El Niño events contribute to enhance the long-term freshening trend (up to 30%) in the far western equatorial Pacific and moderately reduce that freshening (up to 10%) in the South Pacific Convergence Zone (SPCZ). Our results thus suggest that the observed eastward expansion of the surface covered by low-salinity waters in the western half of the tropical Pacific is mostly due to climate change rather than to the documented possible increased occurrence and intensity of CP El Niño events. The sensitivity of the trend estimates to the different periodicity of the SSS data records is also discussed. **Citation:** Singh, A., and T. Delcroix (2011), Estimating the effects of ENSO upon the observed freshening trends of the western tropical Pacific Ocean, *Geophys. Res. Lett.*, *38*, L21607, doi:10.1029/2011GL049636.

1. Introduction

[2] Estimates from a variety of data sources indicate that Sea Surface Temperature (SST) in the tropics and subtropics has increased by 0.4 to 1°C over the last 100 years [e.g., *Deser et al.*, 2010]. It is now unequivocal that causes of this warming trend are for the most part human activities which increase the amount of greenhouse gases in the atmosphere [*Intergovernmental Panel on Climate Change*, 2007]. Focusing on the tropical Pacific, the amplitude of that SST trend however differs from one region to another, and it was further shown to be sensitive to the used dataset and data span, as well as to the way low-frequency modes such as ENSO (El Niño Southern Oscillation) are considered (or not) in the computation. This proves especially visible in the eastern-central equatorial Pacific, the region of maximum ENSO variability in SST, where even the sign of the SST trend can vary depending on different data products and data processing [e.g., *Cravatte et al.*, 2009, Table 1; *Deser et al.*, 2010, Figure 1; *Compo and Sardeshmukh*, 2010, Figure 8].

[3] Estimates of Sea Surface Salinity (SSS) trends are much less numerous than for SST, reflecting the relative paucity of in situ observations and the present shortness of the SMOS (Soil Moisture and Ocean Salinity) remotely-sensed SSS records. Yet, in the tropical Pacific, all studies analyzing multi-decadal SSS records (>30 years) agree on a freshening trend of the order of −0.1 to −0.4 pss over the last 50 years in the heavy precipitation regions of western Pacific warm pool and in the Inter-Tropical and South Pacific Convergence Zones (ITCZ and SPCZ, respectively [*Delcroix et al.*, 2007; *Cravatte et al.*, 2009; *Durack and Wijffels*, 2010; *Terray et al.*, 2011]. Interestingly, this freshening trend can be ascribed to climate change as it is found consistent with the expectation of a mean hydrological cycle increase in a warming world, in line with the wet-get-wetter paradigm [*Held and Soden*, 2006; *Cravatte et al.*, 2009; *Terray et al.*, 2011].

[4] The western Pacific warm pool and the SPCZ regions (and the ITCZ to a less extent), where we observed maximum freshening trends, are also regions of highest ENSO variability in SSS, with peak to peak anomalies of the order of 1 pss between El Niño and La Niña events [*Delcroix and Hénin*, 1991]. This raises the question as to what extent have fluctuations in the timing, amplitude, number, as well as the asymmetry of El Niño and La Niña events contributed, if any, to the observed freshening trend. That question is particularly relevant these days with the recent enhanced attention given to the two flavours of ENSO events, hereafter called Eastern and Central Pacific (EP and CP, respectively) ENSO, which have different signatures in SSS [*Singh et al.*, 2011] and were shown to potentially affect the interpretation of long-term trends in SST [*Lee and McPhaden*, 2010]. To answer the question, our study thus attempts to quantify the ENSO effects on long-term trends in SSS, as a possible input to the broad question of how to discriminate natural climate variability from mean climate change. The rest of the manuscript is organized as follows: section 2 describes the data and methods used to discriminate the EP and CP ENSO signature from long-term trends; section 3 describes the results; and a conclusion and discussion appear in section 4.

2. Data and Methods

[5] The SSS data were obtained from the 1° longitude by 1° latitude and 1 month gridded product of *Delcroix et al.* [2011] for the tropical Pacific region (30°S–30°N, 120°E–70°W) and from 1950 to 2008. Each grid point has an associated error indicating the confidence we can have on the SSS product. This error is given as a percentage of the interannual variance at that point. When there is no SSS data

[1]LEGOS, UMR 5566, CNES, CNRS, IRD, Université de Toulouse, Toulouse, France.

0094-8276/11/2011GL049636

available, the error is 100% and the SSS gridded value is equal to the monthly mean climatological SSS. Following *Singh et al.* [2011], we consider that we can trust the SSS gridded product value if the error is less than the 80% threshold.

[6] Various techniques have been used to discriminate the ENSO component from the long-term variability (assumed to be best represented by a linear trend). Maybe the most frequently used method to capture the ENSO component is based on least squares linear regression, lagged or not, onto ENSO indices. Some of the indices we found in the literature include the Southern Oscillation Index (SOI), the NINO3 or NINO4 SST anomalies, and the principal component(s) of Empirical Orthogonal Function (EOF) or Principal Oscillation Patterns (POP) analyses on tropical Pacific SST or 3-dimensional temperature, some indices being previously band-pass filtered [*Jones*, 1989; *Kelly and Jones*, 1996; *Cane et al.*, 1997; *Latif et al.*, 1997; *Santer et al.*, 2001; *Solomon and Newman*, 2011]. Other methods involve band-pass filters isolating ENSO periods (approximately within 2 to 7 years), so-called dynamic or thermodynamic models, and trend EOF analysis [*Lau and Weng*, 1999; *Compo and Sardeshmukh*, 2010; *Thompson et al.*, 2009; *Barbosa and Andersen*, 2009]. The long-term variability is then estimated by computing linear trends on the difference between the original record and the natural (ENSO) component(s). None of these methods are fully satisfactory [see *Compo and Sardeshmukh*, 2010]. Also, at the time of writing, none of the authors have diagnosed the respective impacts of the EP and CP ENSO on long term trends, with the exception of *Lee and McPhaden* [2010] who compared linear trends in SST for the eastern (NINO3) and western (NINO4) Pacific regions, respectively.

[7] For the sake of simplicity, we choose to use a simple multivariate least squares linear regression technique to isolate the respective effects of EP and CP ENSO on SSS from the long term variability. To distinguish between the EP and CP ENSO, we use the Niño Cold Tongue (N_{CT}) and Niño Warm Pool (N_{WP}) ENSO indices recently derived by *Ren and Jin* [2011]. As discussed by these authors, these new indices are the best suited to discriminate between EP and CP ENSO, especially because they are almost orthogonal in contrast to the NIÑO3 and NIÑO4 SST indices. SSS anomalies (SSSA) and N_{CT} and N_{WP} indices were first calculated relative to the 1971–2000 mean monthly climatology. The SSSA time series at each grid point (x,y) were then regressed onto a linear function of time, N_{CT} and N_{WP} for the period 1955–2008, using the following equation:

$$\underbrace{SSSA_{x,y}(t)}_{\mathrm{I}} = \underbrace{\alpha_{x,y}.t}_{\mathrm{II}} + \underbrace{\beta_{x,y}.N_{CT}(t-\Delta t)}_{\mathrm{III}} + \underbrace{\gamma_{x,y}.N_{WP}(t-\Delta t)}_{\mathrm{IV}} + \underbrace{\xi_{x,y}}_{\mathrm{V}} \quad (1)$$

where α, β, and γ are the coefficients obtained after regressing SSSA onto time t, N_{CT} and N_{WP}, respectively, Δt represents the lag between SSSA and the ENSO indices, and ξ is the residual obtained from the multivariate regression analysis. The lag Δt was derived from the analysis of *Delcroix* [1998] showing that the ENSO signature in SSS lags the one in SST by about 3 months; sensitivity tests show that using different Δt from 0 to 6 months does not significantly change our results. Trends at each grid point were then calculated for terms I to V in equation (1), which we will refer to as the overall, non-ENSO, EP-ENSO, CP-ENSO, and residual trends, respectively. The calculation of trends were made following the works of *Harrison and Carson* [2007] and *Cravatte et al.* [2009] to ensure that data with large errors did not significantly affect the final result. In brief, we computed the linear trends only for the grid points that contain at least five 'good' SSS values (with less than 80% associated error) in each of at least 8 of the 11 pentads since 1955, starting from [1955–1959], and 7 of the 10 shifted pentads since 1958, starting from [1958–1962]. The significances of the trends were estimated at the 95% confidence level based on a Student's *t*-test.

3. Results

[8] As an illustration, Figure 1d shows the combined effects of ENSO events and long-term trends on SSS changes in the western equatorial Pacific (2°N–2°S, 150°E–170°W). In general, we observe a SSS decrease during El Niño events (negative SOI; Figure 1a) and a SSS increase during La Niña events (positive SOI), together with a long-term freshening trend of the order of −0.16 pss/50 years. (The correlation coefficient between the SSS time series and the SOI is R = 0.84 at zero lag). Figures 1b and 1c further show the relative amplitude and the timing of the EP and CP types of ENSO, as indicated by the N_{CT} and N_{WP} indices. For instance, the N_{CT} index peaks with magnitude of 2.1°C during the very strong EP El Niño episode of 1997–98, while the N_{WP} index remains close to zero; in comparison, the N_{WP} index peaks with magnitude of 0.7°C during the CP El Niño episode of 2002–04, while the N_{CT} index remains close to zero. In both instances, we observe a SSS freshening of the order of −0.25 pss. As discussed by *Singh et al.* [2011] and below, this reflects that both EP and CP El Niño events affect the western equatorial Pacific, noting that the EP El Niño events mostly affect the eastern half of that region and the CP ENSO the western half. Also shown in Figure 1e is the time series of the averaged normalized SSS errors (se), indicating that the lack of interannual SSS variability at the beginning of the time series is spurious and actually reflects a poor data distribution (se > 80%).

[9] Values of the β and γ regression coefficients in equation (1), denoting the EP and CP ENSO signature in SSS, respectively, are shown in Figure 2. (Note that β and γ are not significantly modified when the N_{CT} and N_{WP} are band-pass filtered in the 2–7 year ENSO band.) Generally, Figure 2 indicates a decrease of SSS in the western equatorial Pacific and in the ITCZ, and an increase of SSS in the SPCZ, during both EP and CP El Niño events, and vice versa during La Niña events. These El Niño SSS changes mostly result from the anomalous eastward advection of low-salinity warm pool waters in the equatorial band, and a rainfall deficit related to the north-eastward displacement of the SPCZ [e.g., *Delcroix and Picaut*, 1998; *Gouriou and Delcroix*, 2002]. The SSS decrease in the equatorial region, centered near the dateline during EP El Niño events, is however shifted about ~15° in longitude westward and strengthened in magnitude during CP El Niño events. Moreover, the SSS increase in the SPCZ is somewhat reduced during CP El Niño events with a spatial signature inclined more to the southwest, as compared to EP El Niño events (note that the amplitude of N_{WP} is about 75% smaller

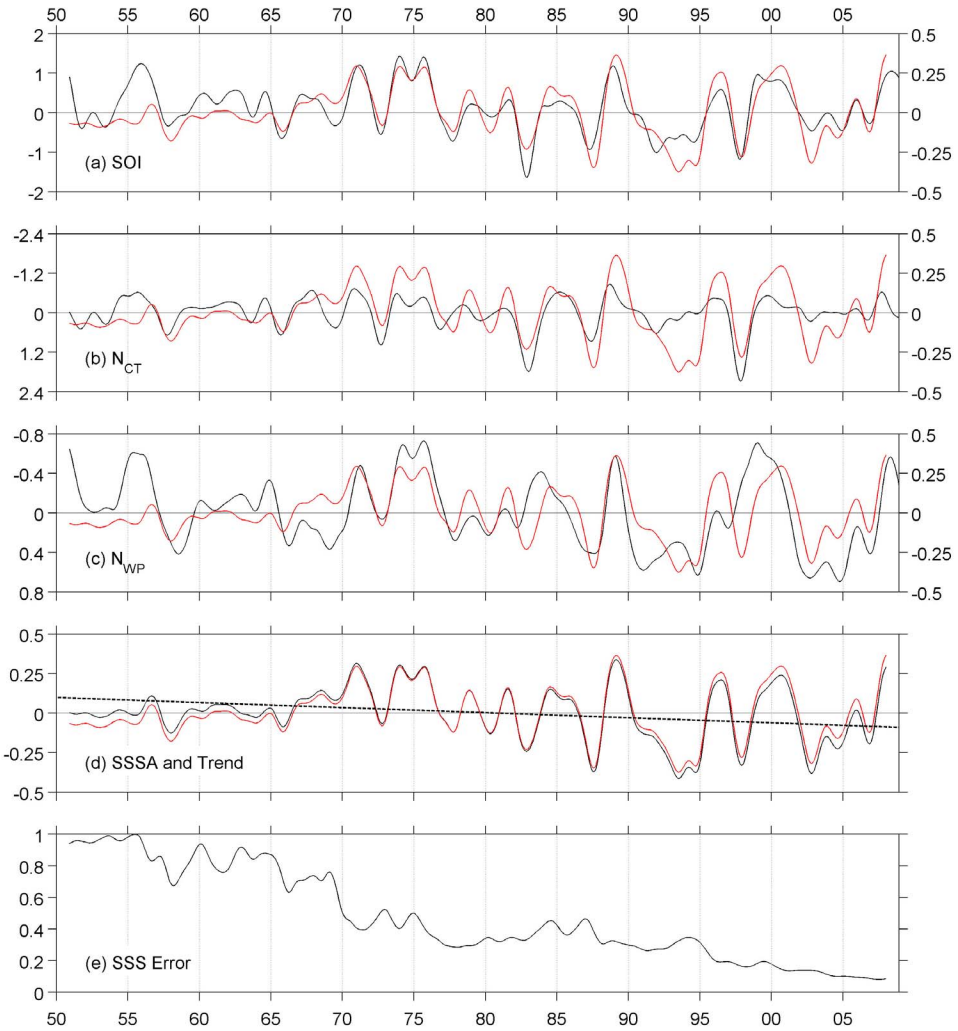

Figure 1. Time series of the (a) Southern Oscillation Index (SOI), (b) ENSO Cold Tongue Index (N_{CT}), (c) ENSO Warm Pool Index (N_{WP}), (d) SSS anomalies and linear trend, and (e) normalized SSS errors for the 1950–2008 period (black curves). Detrended SSS anomalies are scaled on the right vertical scales in Figures 1a–1c and on the left in Figure 1d (red curves). The SSS anomalies and errors were averaged in the region 150°E–170°W and 2°S–2°N. Anomalies in Figures 1a–1d are relative to the 1971–2000 mean monthly climatology. Values in Figures 1a–1e are smoothed using a 25-months Hanning filter for clarity. The SSS trend in Figure 1d, significant at the 95% confidence level, was computed over 1955–2008 ignoring values with SSS error greater than 0.8. Units are degree Celsius in Figures 1b and 1c, pss in Figure 1d, and percent divided by 100 in Figure 1e. Note the different and reversed vertical scales in temperature in Figures 1b and 1c.

than the amplitude of N_{CT}, see Figures 1b and 1c). These EP and CP ENSO SSS changes are remarkably consistent with those documented by *Singh et al.* [2011] from a more sophisticated AHC (Agglomerative Hierarchical Clustering) method, reinforcing our confidence in using our simple regression analysis. As discussed by these last authors, the SSS changes during CP as compared to EP El Niño events reflect a reduced eastward advection of low-salinity warm

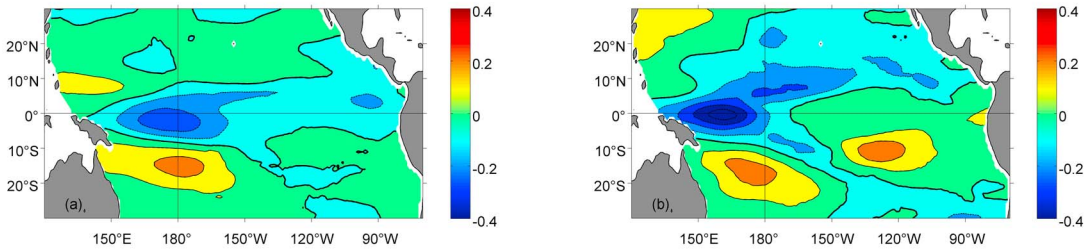

Figure 2. Coefficient estimates (a) β and (b) γ after regressing SSS anomalies with unfiltered N_{CT} and N_{WP} indices leading by 3 months, respectively (see equation (1)). Negative values thus indicate a decrease of SSS during EP or CP El Niño events and vice versa during La Niña events. Units are in pss/°C.

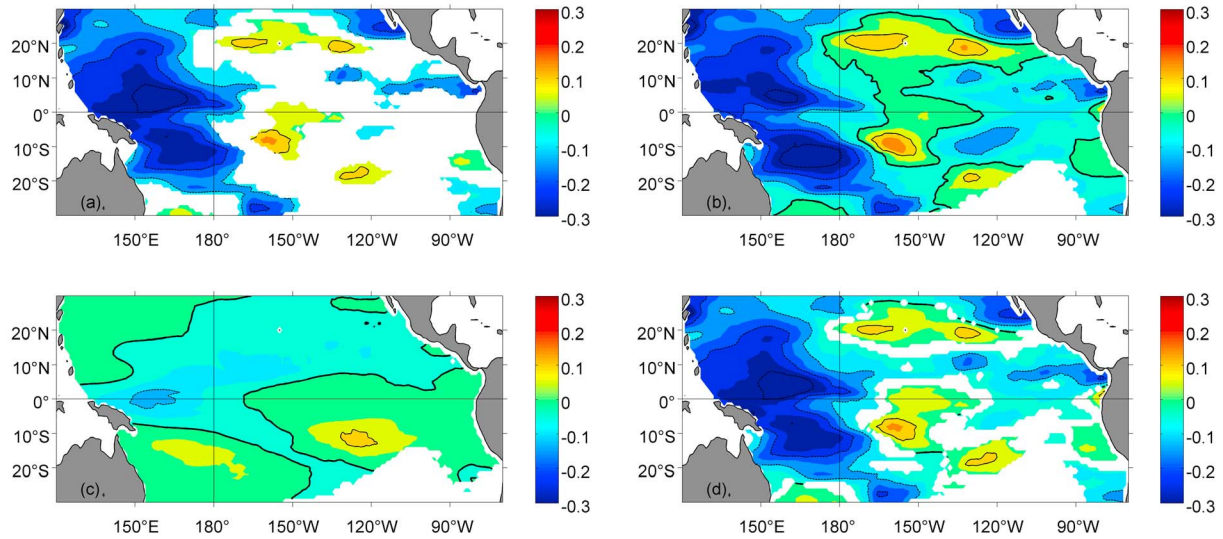

Figure 3. Linear trends in SSS anomalies over the 1955–2008 period due to (a) overall long-term variability, (b) non-ENSO long-term variability, (c) CP ENSO, and (d) EP and CP ENSO and non-ENSO long term variability (see equation (1)). Units are pss/50 years. Regions where the linear trends are not calculated due to poor data density or are not significant at the 95% confidence level are shaded in white. Thick black contour lines denote the 0 line.

pool waters in the equatorial band, and a reduced northeastward shift of the SPCZ and associated precipitation changes.

[10] The trends obtained from terms I (overall trend), II (non-ENSO trend) and IV (CP ENSO trend) in equation (1) are shown in Figures 3a–3c, respectively. The trends obtained from terms III (EP ENSO trend) and V (residual trend) are not shown because they are one order of magnitude smaller than the other terms and both are not significant at the 95% confidence level. The overall trend (Figure 3a) shows maximum freshening concentrated in the western Pacific warm pool, including the SPCZ, with magnitudes of the order of −0.1 to −0.4 pss/50 years. Some freshening (maximum −0.22 pss/50 years) is also visible under the ITCZ in the eastern Pacific, and there is a hint for a saltening trend in the high SSS regions of the Hawaiian and French Polynesia archipelago (with maxima reaching 0.14 and 0.16 pss/50 years, respectively), consistent with the dry-get-drier paradigm. These overall trends compare quite well in space with those determined by *Cravatte et al.* [2009] and *Durack and Wijffels* [2010] although they slightly differ in magnitude, probably due to the different periods of analysis (see the discussion of Figure 4 in Section IV). Aside from a probable influence of ocean dynamics [see *Huang et al.*, 2005], these SSS trends are qualitatively consistent with satellite-derived estimates of P-E trends [*Wentz et al.*, 2007]

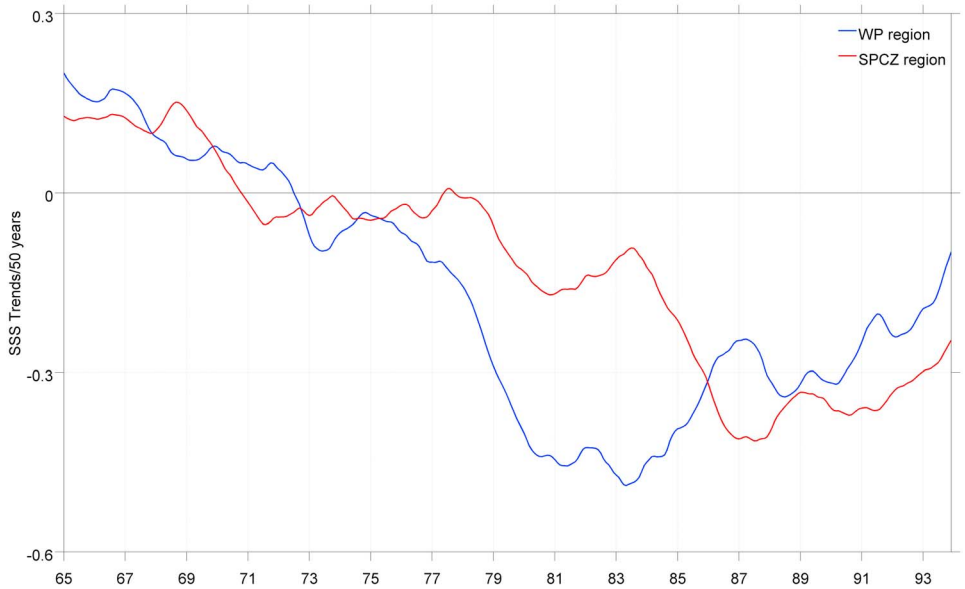

Figure 4. 30-years running trends of mean SSS anomalies in the warm pool (150°E–170°W, 5°S–10°N; in blue) and SPCZ (150°E–170°W, 20°S–5°S; in red) regions over the 1950–2008 period. Units are pss/50 years.

Table 1. Mean Trend Values (Computed Over 1955–2008 and Expressed in pss/50 Years) of the Reconstructed and Overall SSS anomalies in the pool (WP), SPCZ, and ITCZ Regions

	Region	CP ENSO	Non-ENSO	(EP + CP) ENSO + Non-ENSO	Overall
WP	150°E–170°W, 5°S–10°N	−0.06	−0.14	−0.21	−0.21
SPCZ	150°E–170°W, 20°S–5°S	+0.02	−0.22	−0.19	−0.20
ITCZ	150°W–90°W, 5°N–15°N	−0.02	−0.04	−0.07	−0.10

and with most of the P trends derived from rain gauge data recorded in the Pacific Islands (figures not shown).

[11] Figure 3d shows the trends from the reconstructed SSSA using the right hand side terms of equation (1) minus the residuals, ξ. The pattern and magnitude of the trends are very similar to those in Figure 3a confirming the non-significant effect of the residual trend as well as the reliability of equation (1) in efficiently extracting the main signals. The non-ENSO trend (Figure 3b) does resemble the overall trend (Figure 3a), with however some differences in amplitude, and an extension of the regions where the confidence intervals exceed 95%. The differences in amplitude are chiefly located in the far western equatorial Pacific and in the SPCZ and ITCZ regions and can largely be explained by the CP ENSO component of the trend (Figure 3c), qualitatively similar to the CP ENSO SSS pattern (Figure 2b) by construction. Noteworthy, CP ENSO events thus have a tendency to enhance the non-ENSO freshening trend in the far western equatorial Pacific and ITCZ regions (by about 30% and 20%, respectively), and to reduce the non-ENSO freshening trend in the SPCZ region (by about 10%). The 30% enhanced SSS freshening in the far western equatorial Pacific is comparable in magnitude to the 30–40% enhanced SST warming in the eastern equatorial Pacific due to ENSO [*Compo and Sardeshmukh*, 2010]. A quantification of mean trend values for different terms and regions are given in Table 1 for SSS.

4. Conclusion and Discussion

[12] The El Niño events generally result in a decrease of SSS in the western half of the equatorial Pacific, and an increase of SSS in the SPCZ mean area (and vice versa during La Niña events), mainly in relation to the import of low-salinity waters from the west in the equatorial band and to a rainfall deficit in the SPCZ mean area. The EP and CP types of ENSO events have however distinct quantitative impact on SSS [*Singh et al.*, 2011]. In brief, the CP El Niño events are characterised by a westward shift (15° longitude) of the maximum SSS decrease in the equatorial band, and a reduced (50%) SSS increase in the SPCZ, as compared to EP El Niño events. In addition to the ENSO signal, there is a long-term SSS freshening trend in the precipitation-dominated regions of the western equatorial Pacific and of the SPCZ over the last 50 years, in qualitative agreement with the expected hydrological cycle increase in a warming world [*Cravatte et al.*, 2009]. The aim of our study was thus to estimate the EP and CP ENSO contribution to the long-term SSS trends observed in the tropical Pacific.

[13] To tackle the problem, we used in situ SSS data covering the 1955–2008 period, and developed a multivariable regression analysis to discriminate ENSO and non-ENSO trends. We gain confidence in the simple regression analysis as it corroborates the different impacts of the EP and CP ENSO on SSS obtained previously from a more sophisticated technique [*Singh et al.*, 2011]. The contribution of the EP type of ENSO to the observed freshening trends was found to be insignificant in the western half of the tropical Pacific. In comparison, the contribution of the CP type of ENSO was found to be significant, and it tends to appreciably enhance (up to 30%) the freshening trends in the far western equatorial Pacific and moderately reduce (up to 10%) those trends under the SPCZ. As a consequence, we can expect that the assumed increased frequency [*Yeh et al.*, 2009] and intensity [*Lee and McPhaden*, 2010] of CP ENSO will strengthen the freshening trend in the far western equatorial Pacific, and lessen it in the SPCZ, in the years to come.

[14] The documented eastward expansion of the surface covered by low-salinity waters in the warm pool and SPCZ regions [*Cravatte et al.*, 2009] is not evident from the ENSO trends. The EP ENSO trend is negligible, likely because EP El Niño events tend to be followed by EP La Niña events [*Kug et al.*, 2009]. In contrast, the CP El Niño events tend not to be followed by CP La Niña events (ibid), so that the long-term effect of CP ENSO actually induces a maximum freshening trend in the *far* western equatorial Pacific and a maximum saltening trend in the SPCZ. Hence, we do not expect the low-salinity waters to expand eastward due to ENSO, suggesting that the observed eastward expansion of low-salinity waters is a sign of climate change rather than just a signature of the increased occurrence, intensity and asymmetrical nature of CP ENSO events.

[15] This study illustrates one possible way of estimating the contribution of the EP and CP ENSO signal to the long-term trend in SSS. It raises a number of issues. Firstly, the statistical analysis we intentionally adopted here for the sake of simplicity is admittedly crude as it is based on regression of SSS onto ENSO indices. It would be interesting to test more sophisticated methods, as by *Compo and Sardeshmukh* [2010], noting however, that these usually assumed that the dynamics of ENSO have remained unchanged, and this is probably not the case for the EP and CP types of ENSO. Secondly, it is worth reminding that linear trends are very sensitive to the time-span over which they are computed. To illustrate that sensitivity with SSS data, 30-years running trends were calculated for the warm pool and SPCZ regions (Figure 4). We use a 30-year period as it has been adopted by the World Meteorological Organization (WMO) to be the standard period for the estimation of climatic normals [*World Meteorological Organization*, 1989]. The trends clearly reflect a saltening before the mid-1970s and a freshening after that time in both regions. It is not clear whether or not the reversed sign of the trends is due to increased data density (e.g., see Figure 1e), the climate shift of the late-1970s [*Trenberth and Stepaniak*, 2001], changes in ENSO property [*Wang and An*, 2001], increased occurrence and/or intensity of CP ENSO over EP ENSO [*Lee and McPhaden*, 2010], and/or phase reversal of the Pacific Decadal Oscillation [*Mantua and Hare*, 2002]. Whatever its causes, this

reversal in the pattern of trends warns us that our present results, although based on rather long record lengths (1955–2008), may change when choosing different time periods. Thirdly, many studies have assumed long term anthropogenic trends to be linear, and this may not be adequate [*Karl et al.*, 2000]. It would still be interesting to make use of piecewise linear trends, as by *Tomé and Miranda* [2004], especially in order to account for climate shifts. As a final comment, there is no doubt that long SSS (and climatic) time series must be pursued in order to ease interpretation of long-term trends from observational data.

[16] **Acknowledgments.** This work is a contribution to the GLOSCAL ESA/SMOS proposal supported by CNES. We benefited from freely available datasets, including gridded SSS field from the French SSS Observation Service (http://www.legos.obs-mip.fr/observations/sss/), the SOI (http://www.cpc.ncep.noaa.gov/data/indices/soi), and the NINO3 and NINO4 SST anomalies (http://www.cpc.ncep.noaa.gov/data/indices/sstoi.indices) from which we derived the EP and CP ENSO indices using the formula from *Ren and Jin* [2011]. We thank our colleagues S. Cravatte and G. Alory for their valuable comments on a draft version of this manuscript. One of us (A.S.) benefits from a PhD grant from IRD.

[17] The Editor thanks an anonymous reviewer for their assistance in evaluating this paper.

References

Barbosa, S. M., and O. B. Andersen (2009), Trend patterns in global sea surface temperature, *Int. J. Climatol.*, *29*, 2049–2055, doi:10.1002/joc.1855.

Cane, M. A., A. C. Clement, A. Kaplan, Y. Kushnir, D. Pozdnyakov, R. Seager, S. E. Zebiak, and R. Murtugudde (1997), Twentieth-century sea surface temperature trends, *Science*, *275*(5302), 957–960, doi:10.1126/science.275.5302.957.

Compo, G. P., and P. D. Sardeshmukh (2010), Removing ENSO-related variations from the climate record, *J. Clim.*, *23*(8), 1957–1978, doi:10.1175/2009JCLI2735.1.

Cravatte, S., T. Delcroix, D. Zhang, M. McPhaden, and J. Leloup (2009), Observed freshening and warming of the western Pacific Warm Pool, *Clim. Dyn.*, *33*(4), 565–589, doi:10.1007/s00382-009-0526-7.

Delcroix, T. (1998), Observed surface oceanic and atmospheric variability in the tropical Pacific at seasonal and ENSO timescales: A tentative overview, *J. Geophys. Res.*, *103*(C9), 18,611–18,633, doi:10.1029/98JC00814.

Delcroix, T., and C. Hénin (1991), Seasonal and interannual variations of sea surface salinity in the tropical Pacific Ocean, *J. Geophys. Res.*, *96*(C12), 22,135–22,150, doi:10.1029/91JC02124.

Delcroix, T., and J. Picaut (1998), Zonal displacement of the western equatorial Pacific "fresh pool," *J. Geophys. Res.*, *103*(C1), 1087–1098, doi:10.1029/97JC01912.

Delcroix, T., S. Cravatte, and M. J. McPhaden (2007), Decadal variations and trends in tropical Pacific sea surface salinity since 1970, *J. Geophys. Res.*, *112*, C03012, doi:10.1029/2006JC003801.

Delcroix, T., G. Alory, S. Cravatte, T. Corrège, and M. J. McPhaden (2011), A gridded sea surface salinity data set for the tropical Pacific with sample applications (1950–2008), *Deep Sea Res., Part I*, *58*(1), 38–48, doi:10.1016/j.dsr.2010.11.002.

Deser, C., A. S. Phillips, and M. A. Alexander (2010), Twentieth century tropical sea surface temperature trends revisited, *Geophys. Res. Lett.*, *37*, L10701, doi:10.1029/2010GL043321.

Durack, P. J., and S. E. Wijffels (2010), Fifty-year trends in global ocean salinities and their relationship to broad-scale warming, *J. Clim.*, *23*(16), 4342–4362, doi:10.1175/2010JCLI3377.1.

Gouriou, Y., and T. Delcroix (2002), Seasonal and ENSO variations of sea surface salinity and temperature in the South Pacific Convergence Zone during 1976–2000, *J. Geophys. Res.*, *107*(C12), 3185, doi:10.1029/2001JC000830.

Harrison, D. E., and M. Carson (2007), Is the world ocean warming? Upper-ocean temperature trends: 1950–2000, *J. Phys. Oceanogr.*, *37*(2), 174–187, doi:10.1175/JPO3005.1.

Held, I. M., and B. J. Soden (2006), Robust responses of the hydrological cycle to global warming, *J. Clim.*, *19*, 5686–5699, doi:10.1175/JCLI3990.1.

Huang, B., V. M. Mehta, and N. Schneider (2005), Oceanic response to idealized net atmospheric freshwater in the Pacific at the decadal time scale, *J. Phys. Oceanogr.*, *35*, 2467–2486, doi:10.1175/JPO2820.1.

Intergovernmental Panel on Climate Change (2007), *Climate Change 2007: Synthesis Report. Contribution of Working Groups I, II and III to the Fourth Assessment Report of the Intergovernmental Panel on Climate Change*, edited by Core Writing Team, R. K. Pachauri, and A. Reisinger, Geneva, Switzerland.

Jones, P. D. (1989), The influence of ENSO on global temperatures, *Clim. Monit*, *17*, 80–89.

Karl, T. R., R. W. Knight, and B. Baker (2000), Evidence for an increase in the rate of global warming?, *Geophys. Res. Lett.*, *27*(5), 719–722, doi:10.1029/1999GL010877.

Kelly, P. M., and P. D. Jones (1996), Removal of the El Niño-Southern Oscillation signal from the gridded surface air temperature data set, *J. Geophys. Res.*, *101*(D14), 19,013–19,022, doi:10.1029/96JD01173.

Kug, J.-S., F.-F. Jin, and S.-I. An (2009), Two types of El Niño events: Cold tongue El Niño and warm pool El Niño, *J. Clim.*, *22*(6), 1499–1515, doi:10.1175/2008JCLI2624.1.

Latif, M., R. Kleeman, and C. Eckert (1997), Greenhouse warming, decadal variability, or El Niño? An attempt to understand the anomalous 1990s, *J. Clim.*, *10*(9), 2221–2239, doi:10.1175/1520-0442(1997)010<2221:GWDVOE>2.0.CO;2.

Lau, K.-M., and H. Weng (1999), Interannual, decadal–interdecadal, and global warming signals in sea surface temperature during 1955–97, *J. Clim.*, *12*(5), 1257–1267, doi:10.1175/1520-0442(1999)012<1257:IDIAGW>2.0.CO;2.

Lee, T., and M. J. McPhaden (2010), Increasing intensity of El Niño in the central-equatorial Pacific, *Geophys. Res. Lett.*, *37*, L14603, doi:10.1029/2010GL044007.

Mantua, N. J., and S. R. Hare (2002), The Pacific Decadal Oscillation, *J. Oceanogr.*, *58*, 35–44, doi:10.1023/A:1015820616384.

Ren, H.-L., and F.-F. Jin (2011), Niño indices for two types of ENSO, *Geophys. Res. Lett.*, *38*, L04704, doi:10.1029/2010GL046031.

Santer, B. D., T. M. L. Wigley, C. Doutriaux, J. S. Boyle, J. E. Hansen, P. D. Jones, G. A. Meehl, E. Roeckner, S. Sengupta, and K. E. Taylor (2001), Accounting for the effects of volcanoes and ENSO in comparisons of modeled and observed temperature trends, *J. Geophys. Res.*, *106*(D22), 28,033–28,059, doi:10.1029/2000JD000189.

Singh, A., T. Delcroix, and S. Cravatte (2011), Contrasting the flavors of El Niño Southern–Oscillation using sea surface salinity observations, *J. Geophys. Res.*, *116*, C06016, doi:10.1029/2010JC006862.

Solomon, A., and M. Newman (2011), Decadal predictability of tropical Indo-Pacific Ocean temperature trends due to anthropogenic forcing in a coupled climate model, *Geophys. Res. Lett.*, *38*, L02703, doi:10.1029/2010GL045978.

Terray, L., L. Corre, S. Cravatte, T. Delcroix, G. Reverdin, and A. Ribes (2011), Near-surface salinity as Nature's rain gauge to detect human influence on the tropical water cycle, *J. Clim.*, doi:10.1175/JCLI-D-10-05025.1.

Thompson, D. W. J., J. M. Wallace, P. D. Jones, and J. J. Kennedy (2009), Identifying signatures of natural climate variability in time series of global-mean surface temperature: Methodology and insights, *J. Clim.*, *22*(22), 6120–6141, doi:10.1175/2009JCLI3089.1.

Tomé, A. R., and P. M. A. Miranda (2004), Piecewise linear fitting and trend changing points of climate parameters, *Geophys. Res. Lett.*, *31*, L02207, doi:10.1029/2003GL019100.

Trenberth, K. E., and D. P. Stepaniak (2001), Indices of El Niño evolution, *J. Clim.*, *14*(8), 1697–1701, doi:10.1175/1520-0442(2001)014<1697:LIOENO>2.0.CO;2.

Wang, B., and S.-I. An (2001), Why the properties of El Niño changed during the late 1970s, *Geophys. Res. Lett.*, *28*(19), 3709–3712, doi:10.1029/2001GL012862.

Wentz, J. F., L. Ricciardulli, K. Hilburn, and C. Mears (2007), How much more rain will global warming bring?, *Science*, *317*(5835), 233–235, doi:10.1126/science.1140746.

World Meteorological Organization (1989), Calculation of monthly and annual 30-year standard normals, *Rep. WCDP 10, WMO-TD 341*, Geneva, Switzerland.

Yeh, S.-W., J.-S. Kug, B. Dewitte, M.-H. Kwon, B. P. Kirtman, and F.-F. Jin (2009), El Niño in a changing climate, *Nature*, *461*(7263), 511–514, doi:10.1038/nature08316.

T. Delcroix and A. Singh, LEGOS, UMR 5566, CNES, CNRS, IRD, Université de Toulouse, 14 av. Edouard Belin, F-31400 Toulouse CEDEX, France. (awnesh.singh@legos.obs-mip.fr)